

Supporting information

In cellulo Synthesis of Dendrimeric Sensors For Fluorescence-on Imaging of Bacterial Phagocytosis

Feng Jiang,^a Yilong Shi,^b Xiaoxue Zou,^a Jiahuai Han,^b Shoufa Han^{a,*}

^aDepartment of Chemical Biology, College of Chemistry and Chemical Engineering, State Key Laboratory for Physical Chemistry of Solid Surfaces, State key Laboratory of Cellular Stress Biology, The Key Laboratory for Chemical Biology of Fujian Province, and The MOE Key Laboratory of Spectrochemical Analysis & Instrumentation, Xiamen University, Xiamen, China;

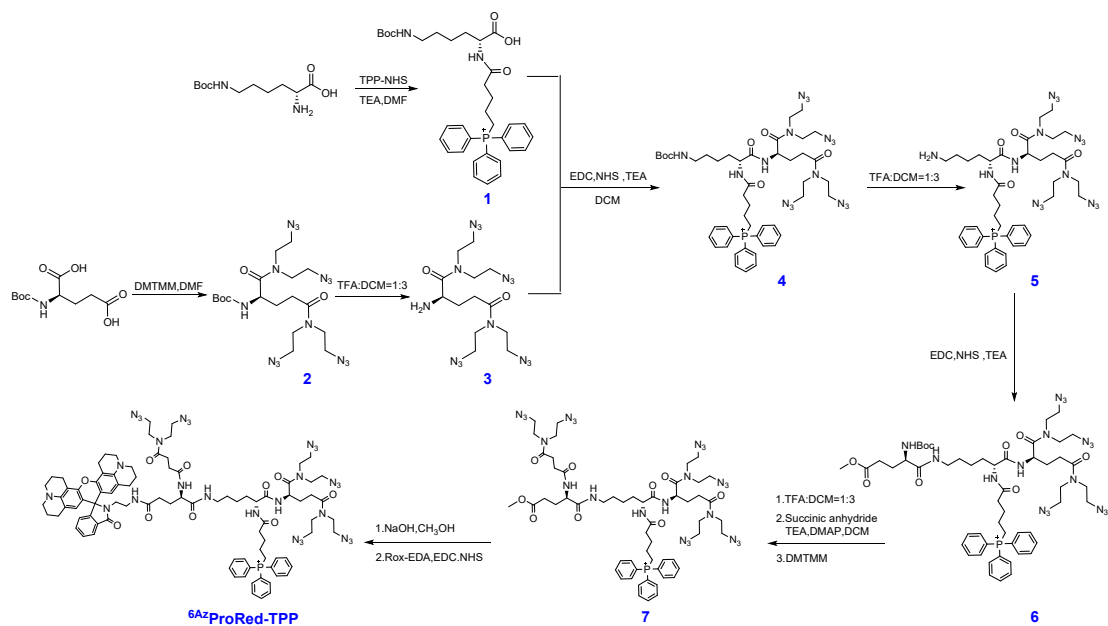
^bState key Laboratory of Cellular Stress Biology, Innovation Center for Cell Signalling Network, School of Life Sciences, Xiamen University;

Corresponding author

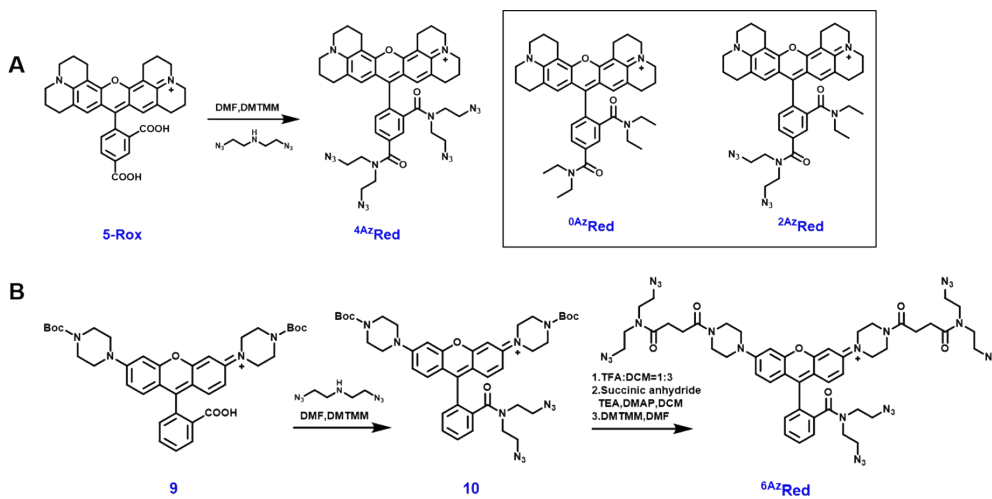
*To whom correspondence should be addressed. E-mail: shoufa@xmu.edu.cn.

CONTENTS

Scheme S1 Synthetic route of ⁶ AzProRed-TPP.....	S3
Scheme S2 Synthetic route of ⁴ AzRed and ⁶ AzRed.....	S3
Fig. S1 In vitro SPAAC of ⁴ AzRed (A), ⁶ AzRed (B) or ⁶ AzProRed-TPP (C) with ^{DBCO} Blue-TPP.....	S4
Fig. S2 Probe targeting for bacteria.....	S5
Fig. S3 Tagging of stressed bacteria with the adduct of ² AzRed and ^{DBCO} Blue-TPP.....	S5
Fig. S4 Tagging of stressed bacteria with the adduct of ⁴ AzRed and ^{DBCO} Blue-TPP.....	S6
Fig. S5 Tagging of stressed bacteria with the adduct of ⁶ AzRed and ^{DBCO} Blue-TPP.....	S6
Fig. S6 Efficiently SPAAC of ² AzRed (A), ⁴ AzRed (B) or ⁶ AzRed (C) and ^{DBCO} Blue-TPP in <i>S.aureus</i>	S7
Fig. S7 Tagging of stressed bacteria with the adduct of ⁰ AzRed and ^{DBCO} Blue-TPP.....	S8
Fig. S8 Colocalization of Dendritic sensors with FITC-D-Lys-labeled bacteria.....	S8
Fig. S9 Optical properties of the adduct of ⁶ AzProRed-TPP and ^{DBCO} Blue-TPP.....	S9
Fig. S10 Tagging of stressed Bacteria with dendritic pH sensors (pH 7.0).	S9
Fig. S11 Tagging <i>S.aureus</i> with Den-pH.....	S9
Fig. S12 Colocalization of Dendritic pH sensors with FITC-D-Lys labelled bacteria.	S10
Fig. S13 The Organelle localization of ⁶ AzProRed-TPP leaked from engulfed bacteria.	S10
Fig. S14 The Organelle localization of ^{DBCO} Blue-TPP.	S10
Fig. S15 Inability of Den-pH to tag <i>S.aureus</i>	S10
NMR spectra.	S11
Mass spectra	S20



Scheme S1 Synthetic route of **6AzProRed-TPP**.



Scheme S2 Synthetic route of **4AzRed** and **6AzRed**.

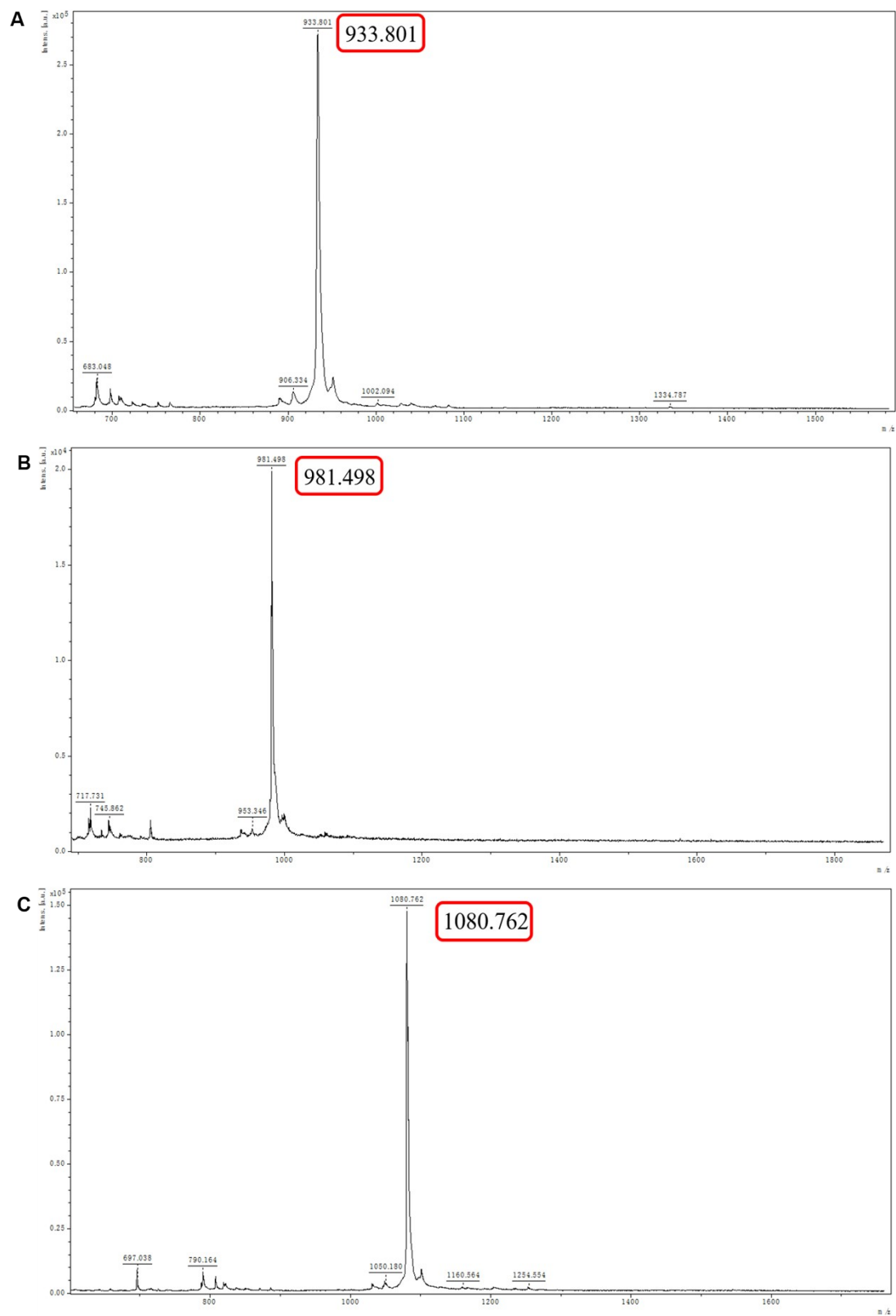


Fig. S1 In vitro SPAAC of ⁴AzRed (A), ⁶AzRed (B) or ⁶AzProRed-TPP (C) with DBCOBlue-TPP.

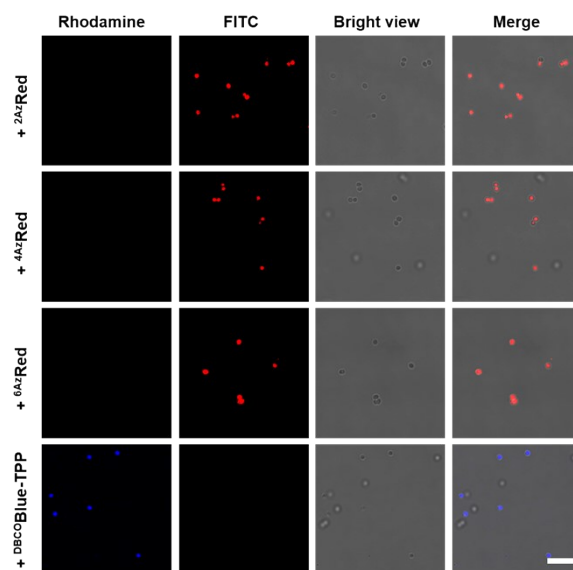


Fig. S2 Probe targeting for bacteria. *S. aureus* were incubated at 37°C for 1 h in LB medium supplemented with ²AzRed (50 μM), ⁴AzRed (50 μM), ⁶AzRed (200 μM) and DBCOBlue-TPP (50 μM) respectively. The *S. aureus* were washed with PBS, and then visualized by confocal microscopy.

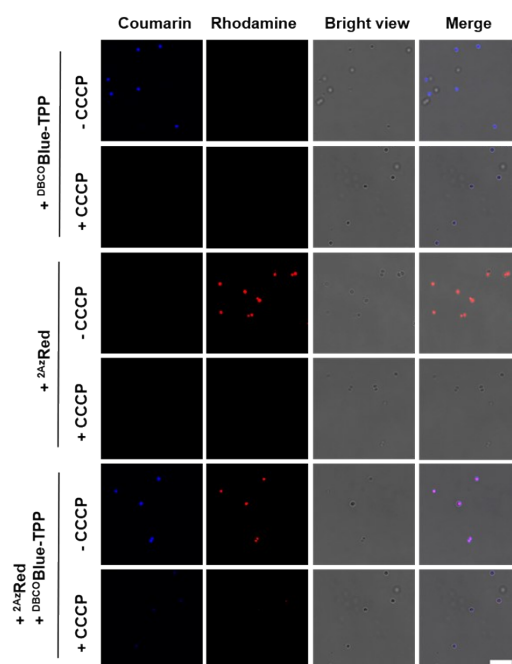


Fig. S3 Tagging of stressed bacteria with the adduct of ²AzRed and DBCOBlue-TPP. *S. aureus* were incubated at 37°C for 1 h in LB medium supplemented with ²AzRed (50 μM) or no addition, and then cultured in LB medium spiked with or without DBCOBlue-TPP (100 μM) for 1 h. *S. aureus* were washed with PBS, and then visualized by confocal microscopy. *S. aureus* were washed with PBS, and then maintained in LB medium containing CCCP (300 μM) for 1 h, and then visualized by confocal microscopy.

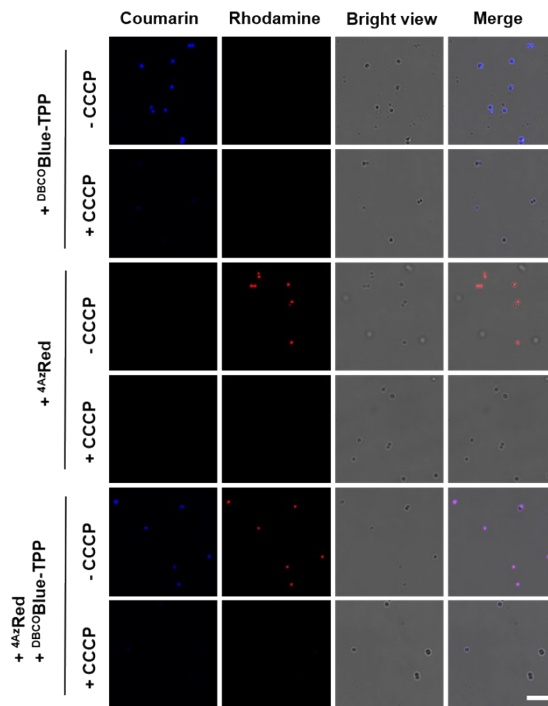


Fig. S4 Tagging of stressed bacteria with the adduct of ⁴AzRed and DBCOBlue-TPP. *S. aureus* were incubated at 37°C for 1 h in LB medium supplemented with ⁴AzRed (50 μM) or no addition, and then cultured in LB medium spiked with or without DBCOBlue-TPP (200 μM) for 1 h. *S. aureus* were washed with PBS, and then visualized by confocal microscopy. *S. aureus* were washed with PBS, and then maintained in LB medium containing CCCP (300 μM) for 1 h, and then visualized by confocal microscopy.

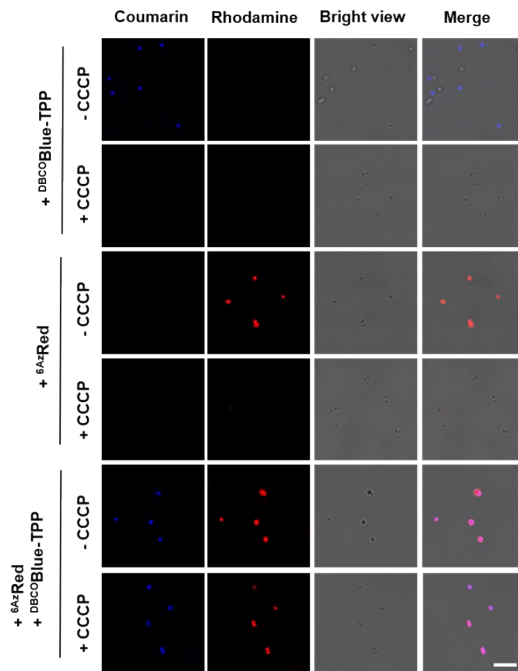


Fig. S5 Tagging of stressed bacteria with the adduct of ⁶AzRed and DBCOBlue-TPP. *S. aureus* were incubated at 37°C for 1 h in LB medium supplemented with ⁶AzRed (200 μM) or no addition, and then cultured in LB medium spiked with or without DBCOBlue-TPP (300 μM) for 1 h. *S. aureus* were washed with PBS, and then visualized by confocal microscopy. *S. aureus* were washed with PBS, and then maintained in LB medium containing CCCP (300 μM) for 1 h, and then visualized by confocal microscopy.

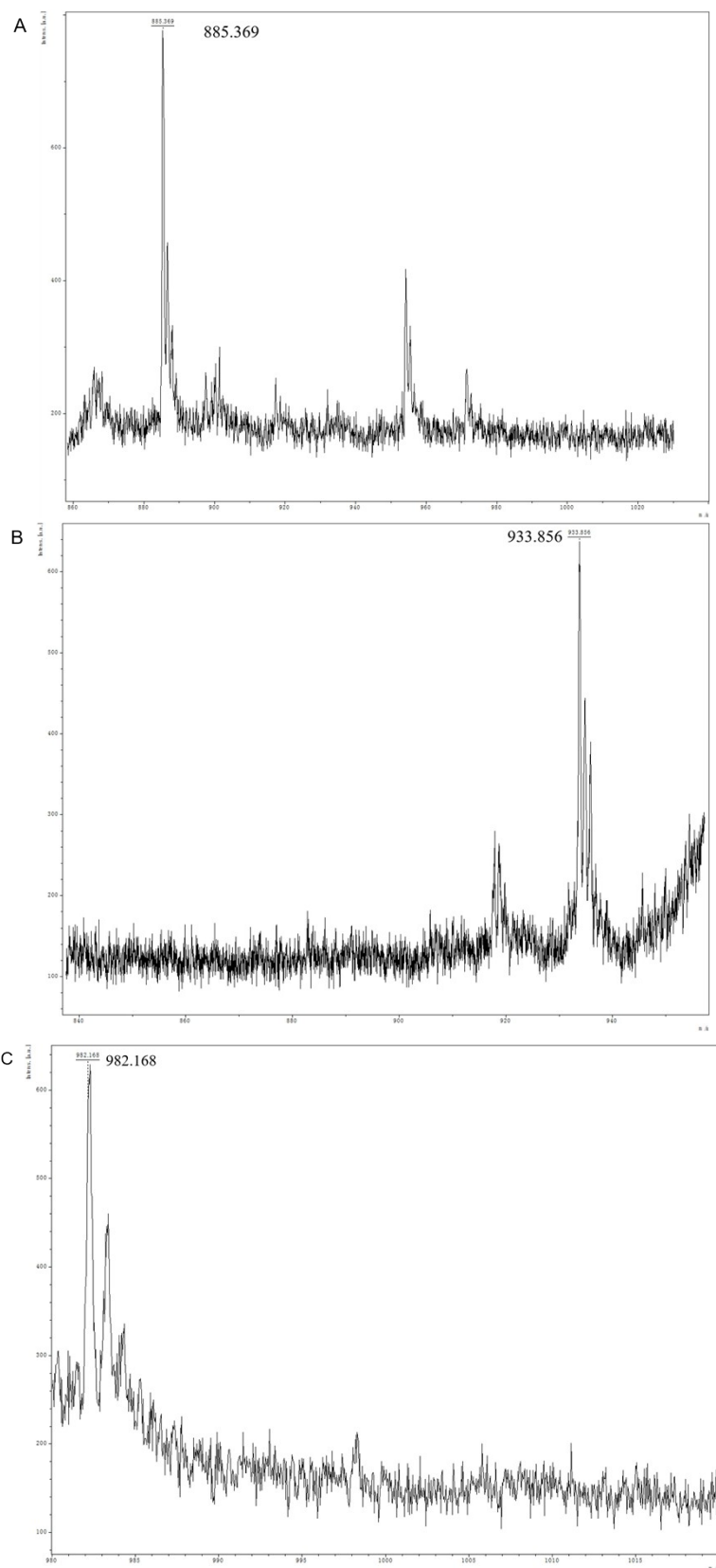


Fig. S6 SPAAC of 2^{Az} Red (A), 4^{Az} Red (B) or 6^{Az} Red (C) and $DBCO^{Blue}$ -TPP in *S. aureus*.

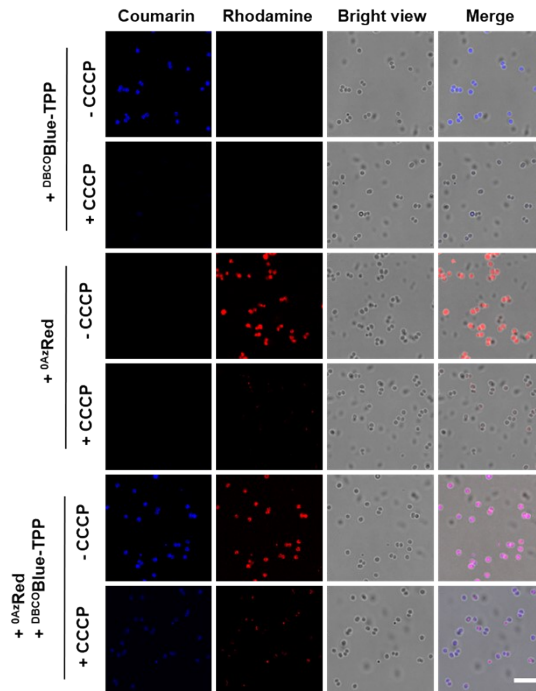


Fig. S7 Tagging of stressed bacteria with the adduct of ⁰AzRed and ^{DBCO}Blue-TPP. *S. aureus* were incubated at 37°C for 1 h in LB medium supplemented with ⁰AzRed (50 μM) or no addition, and then cultured in LB medium spiked with or without ^{DBCO}Blue-TPP (50 μM) for 1 h. *S. aureus* were washed with PBS, and then visualized by confocal microscopy. *S. aureus* were washed with PBS, and then maintained in LB medium containing CCCP (300 μM) for 1 h, and then visualized by confocal microscopy.

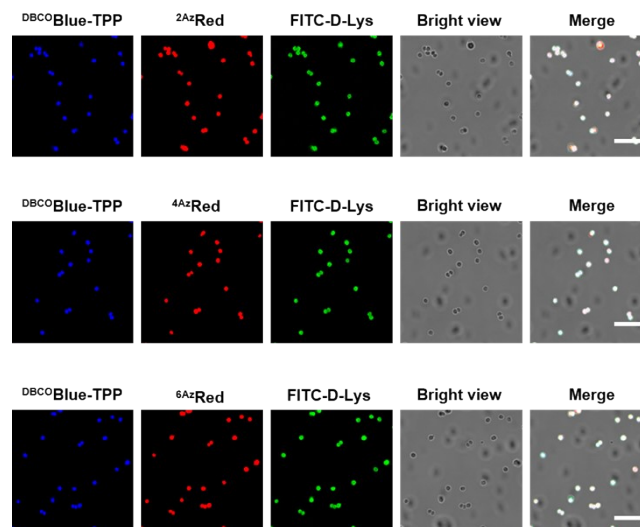


Fig. S8 Colocalization of Dendritic sensors with FITC-D-Lys-labeled bacteria. *S. aureus* prelabeled with FITC-D-Lys were incubated at 37 °C for 1 h in LB medium supplemented with ²AzRed (50 μM), ⁴AzRed (50 μM) and ⁶AzRed (200 μM) respectively, and then cultured in LB medium spiked with ^{DBCO}Blue-TPP (100 μM, 200 μM, 300 μM) for 1 h. The cells were collected, washed with PBS, and then visualized by confocal microscopy

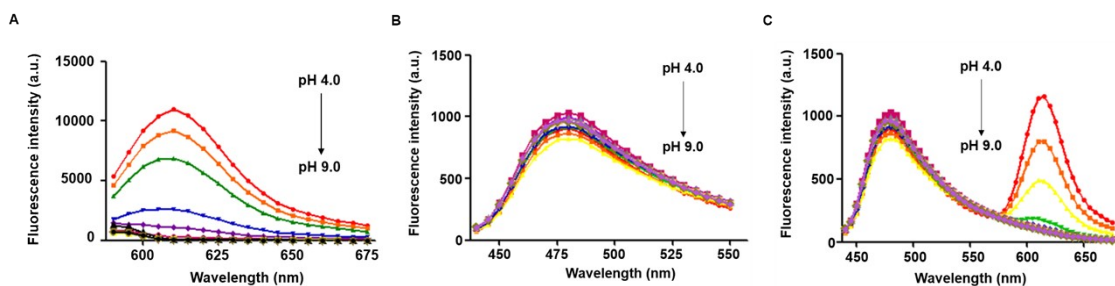


Fig. S9 Optical properties of the adduct of $^{6\text{Az}}\text{ProRed-TPP}$ and DBCOBlue-TPP . (A) Acidity-reporting red fluorescence of $^{6\text{Az}}\text{ProRed-TPP}$. (B) Unaltered blue fluorescence of coumarin in the adduct of $^{6\text{Az}}\text{ProRed-TPP}$ and DBCOBlue-TPP at different pH. (C) pH titration curves of the adducts were plotted using fluorescence emission of coumarin (λ_{475} nm) and Rox(λ_{610} nm) over pH. The adducts were added to PBS buffer (10 mM) of varied pH (4.0–9.0) to a final concentration of 10 μM , and the solutions were analyzed for fluorescence emission using $\lambda_{\text{exc}} = 430$ nm for adducts from $^{6\text{Az}}\text{ProRed-TPP}/\text{DBCOBlue-TPP}$.

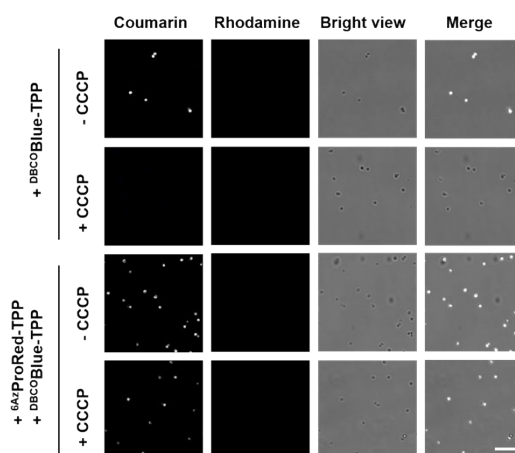


Fig. S10 Tagging of stressed Bacteria with dendritic pH sensors (pH 7.0). *S. aureus* were incubated at 37 °C for 1 h in LB medium supplemented with $^{6\text{Az}}\text{ProRed-TPP}$ (200 μM), and then cultured in LB medium spiked with or without DBCOBlue-TPP (600 μM) for 1 h. *S. aureus* were washed with PBS, and then maintained in buffer of pH 7.0 or buffer of pH 7.0 containing CCCP (300 μM) for 1h, and then visualized by confocal microscopy.

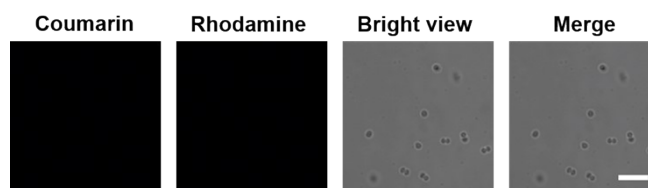


Fig. S11 Inability of Den-pH synthesized in vitro to tag *S. aureus*. *S. aureus* were incubated at 37 °C for 1 h in LB medium supplemented with Den-pH (200 μM) for 1h, and then visualized by confocal microscopy.

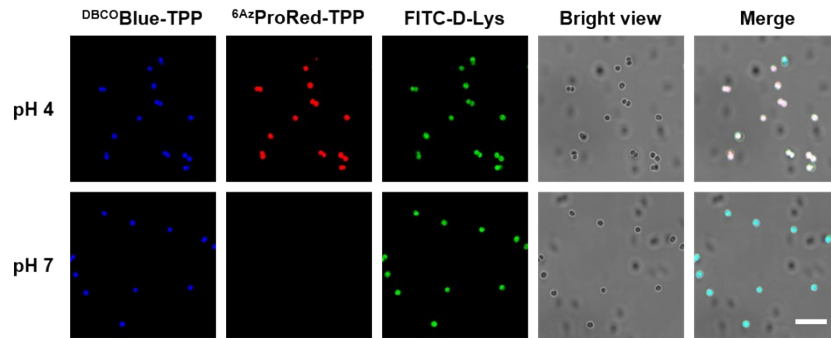


Fig. S12 Colocalization of Dendritic pH sensors with FITC-D-Lys labelled bacteria. *S. aureus* pre-labeled with FITC-D-Lys were incubated at 37 °C for 1 h in LB medium supplemented with ⁶AzProRed-TPP (200 μM), and then cultured in LB medium spiked with DBCOBlue-TPP (300 μM) for 1 h. The cells were collected, washed with PBS, and then maintained in buffer of pH 4.0 or buffer of pH 7.0. The cells were analyzed by confocal fluorescence microscopy.

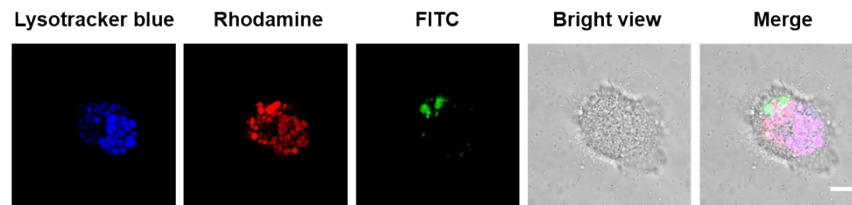


Fig. S13 The Organelle localization of ⁶AzProRed-TPP leaked from engulfed bacteria. *S. aureus* pre-labeled with FITC-D-Lys were incubated with ⁶AzProRed-TPP (200 μM) and DBCOBlue-TPP (600 μM) for 1 h, respectively. The bacteria were co-cultured with BMDMs for 1 h. The BMDM were further treated with lysotracker blue (2 μM) for 30 min, and then visualized by confocal fluorescence microscopy.

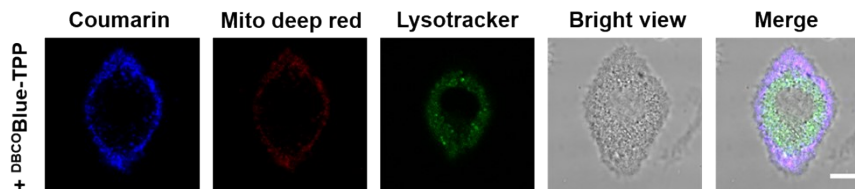


Fig. S14 Organelle localization of DBCOBlue-TPP. BMDMs were incubated with DBCOBlue-TPP (5 μM) for 1 h. BMDMs were further treated with lysotracker green (2 μM) for 1 h, and then with mitotracker deep red (1 μM) for 10 min. The cells visualized by confocal fluorescence microscopy.

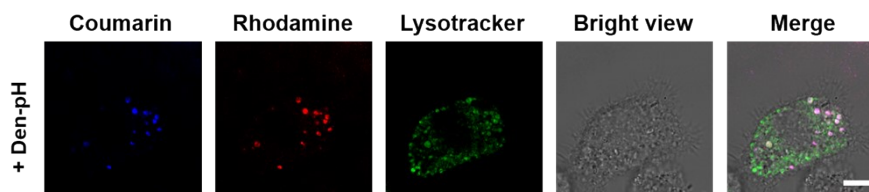


Fig. S15 The Organelle localization of Den-pH. BMDMs were incubated with Den-pH (5 μM) for 1 h. BMDMs were further treated with lysotracker green (2 μM) for 1 h, and then visualized by confocal fluorescence microscopy.

NMR spectra.

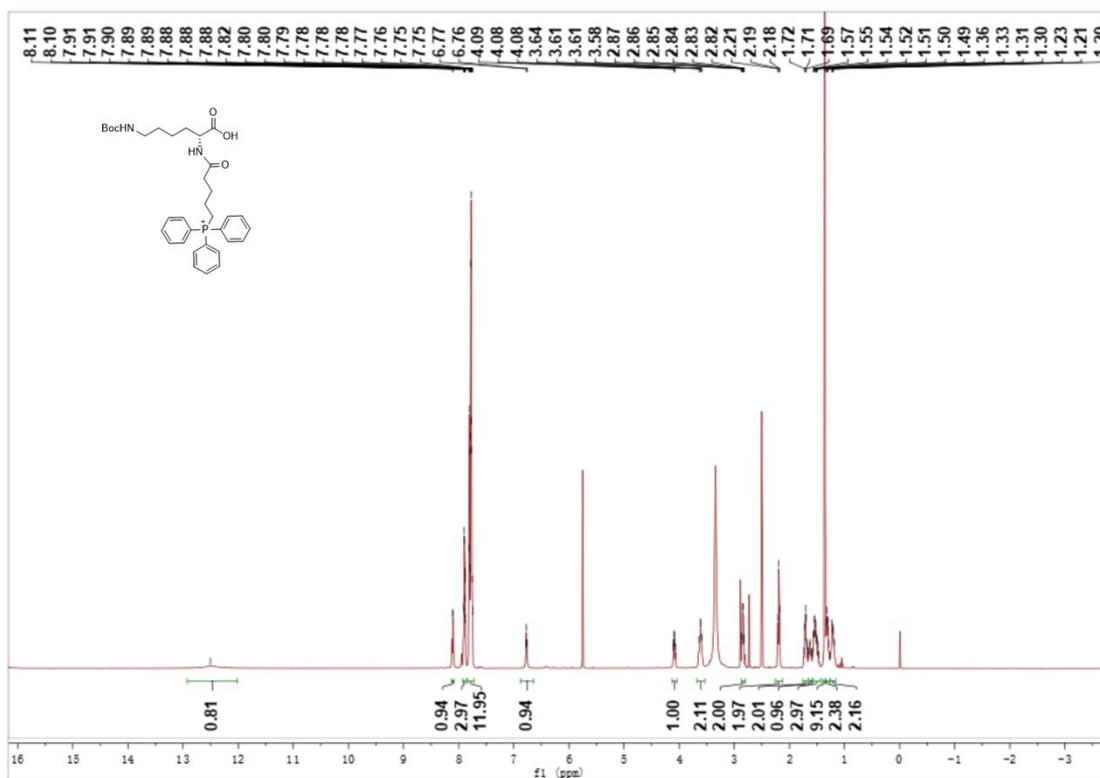


Fig. S11 ^1H NMR spectrum of compound **1** (CDCl_3).

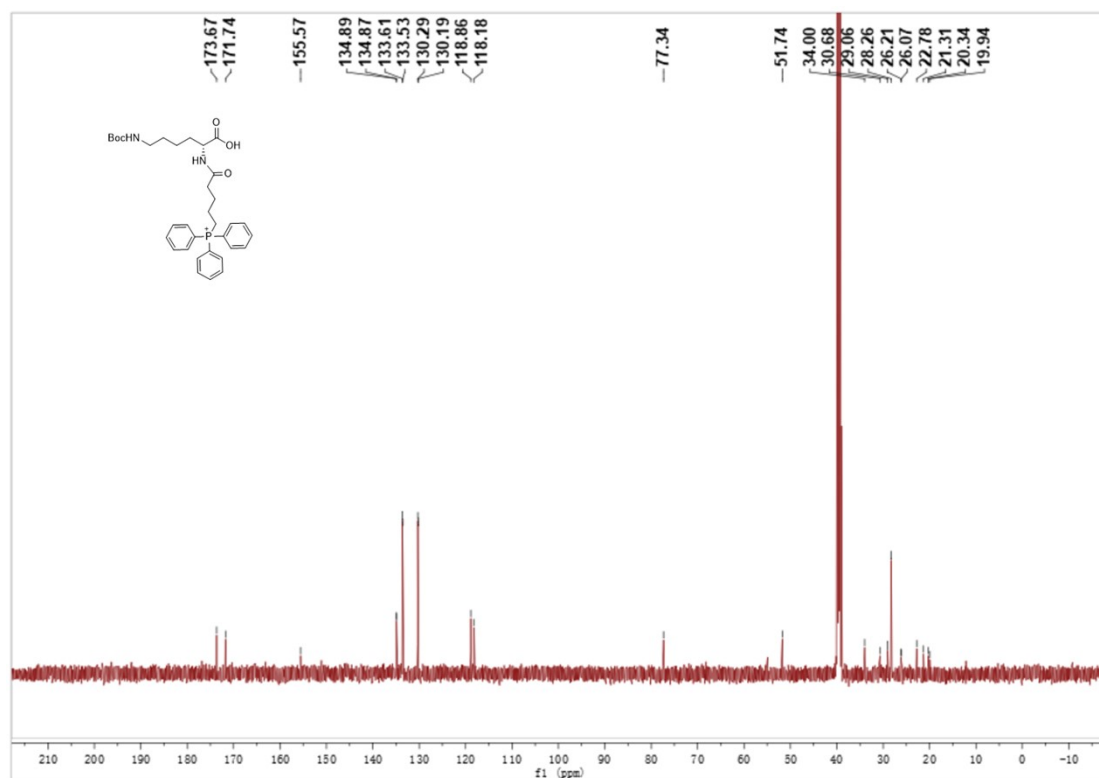


Fig. S12 ^{13}C NMR spectrum of compound **1** (CDCl_3).

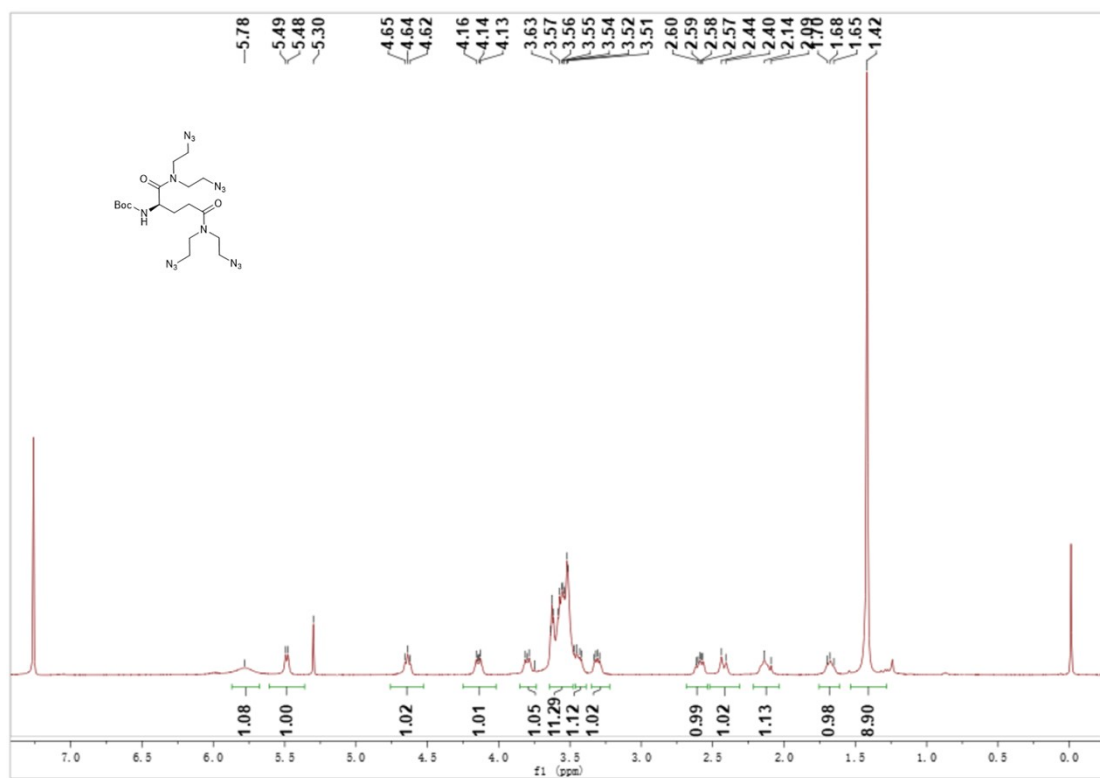


Fig. S13 ¹H NMR spectrum of compound **2** (CDCl₃).

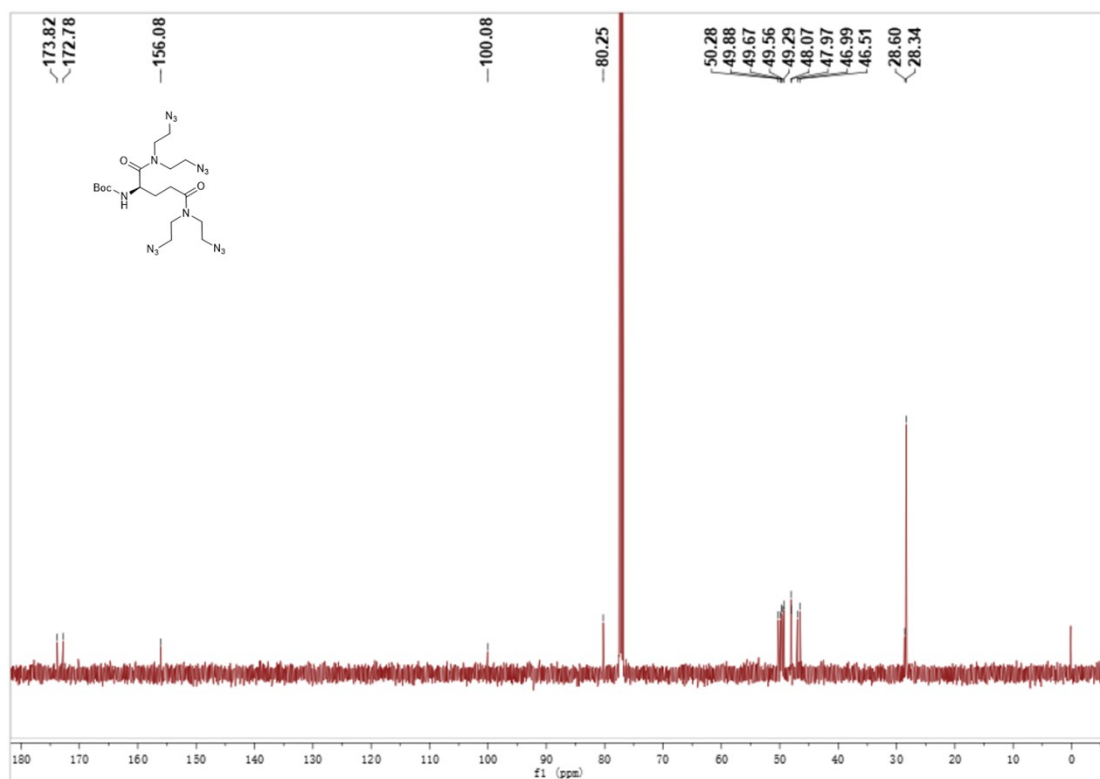


Fig. S14 ¹³C NMR spectrum of compound **2** (CDCl₃).

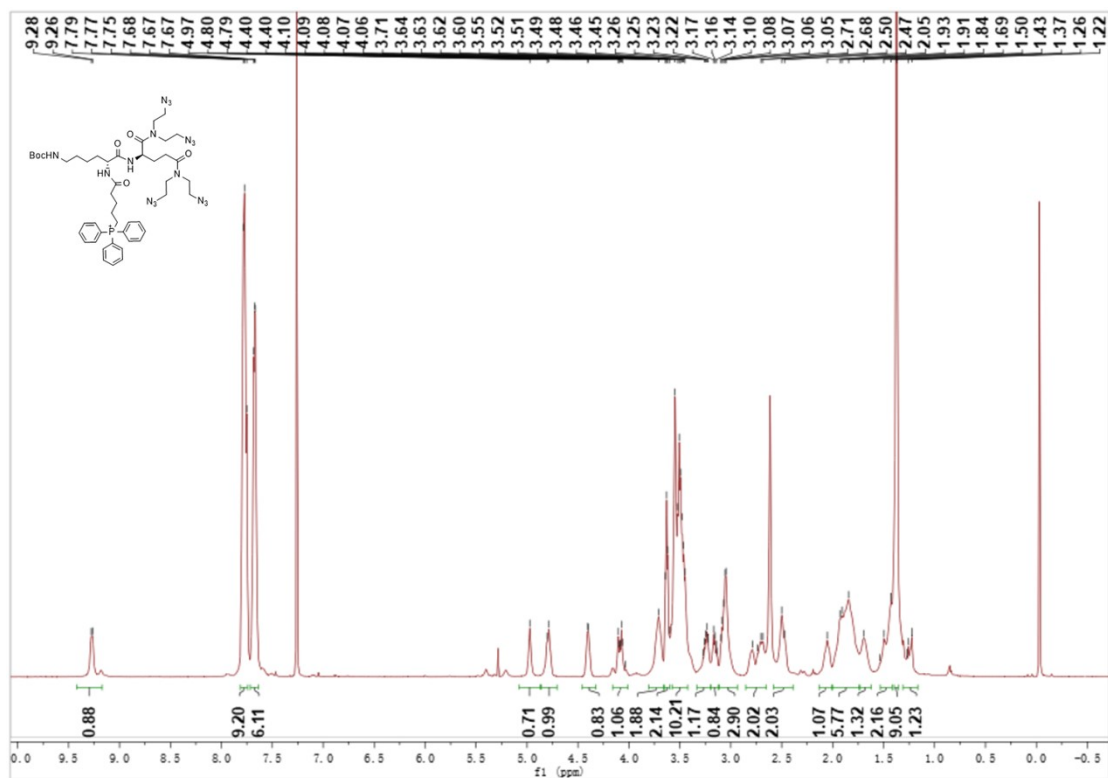


Fig. S15 ^1H NMR spectrum of compound **4** (CDCl_3).

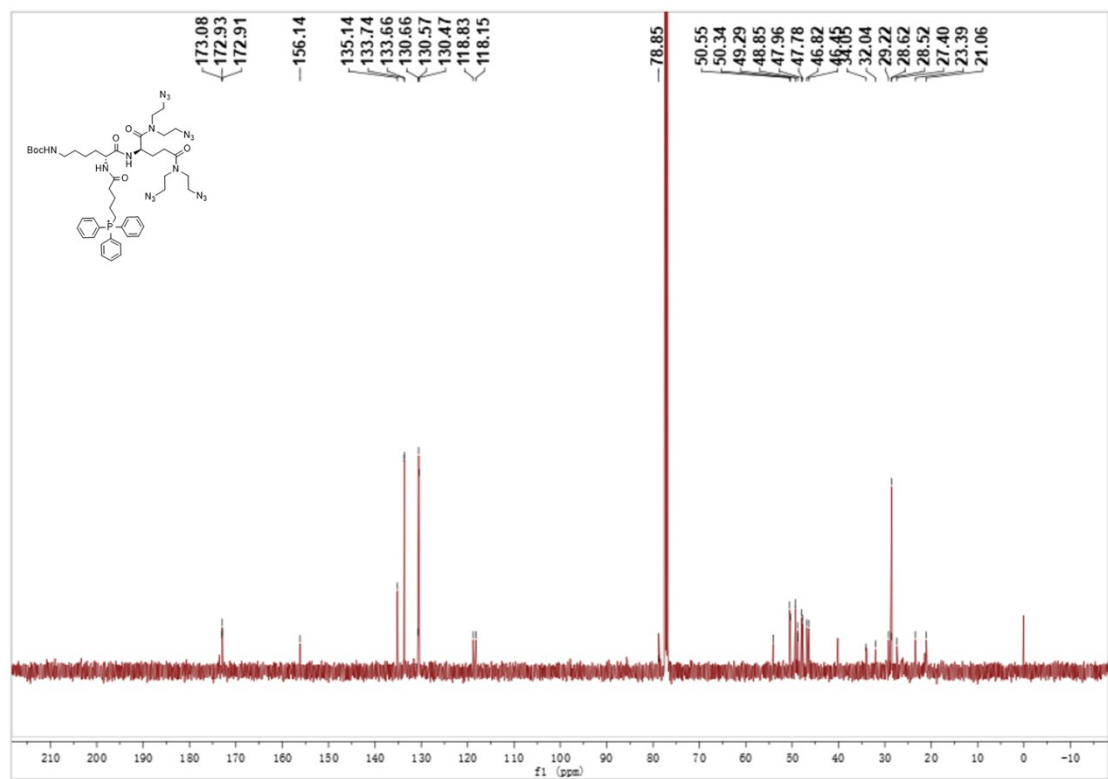


Fig. S16 ^{13}C NMR spectrum of compound **4** (CDCl_3).

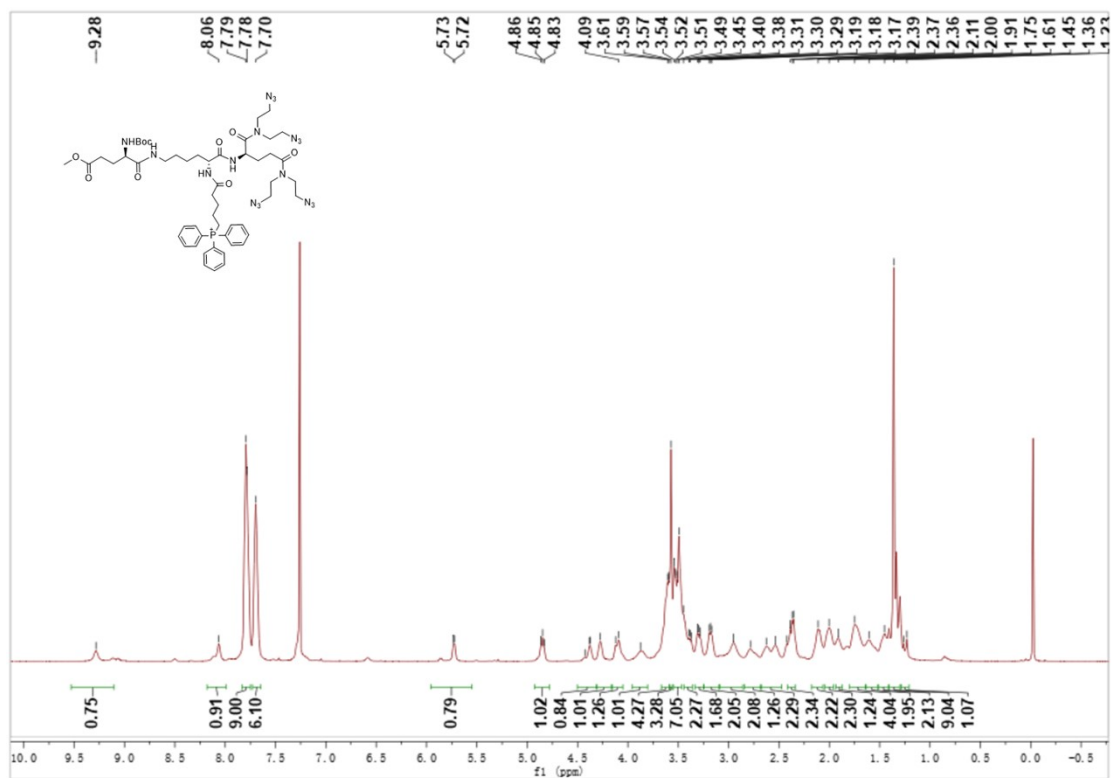


Fig. S17 ^1H NMR spectrum of compound 6 (CDCl_3).

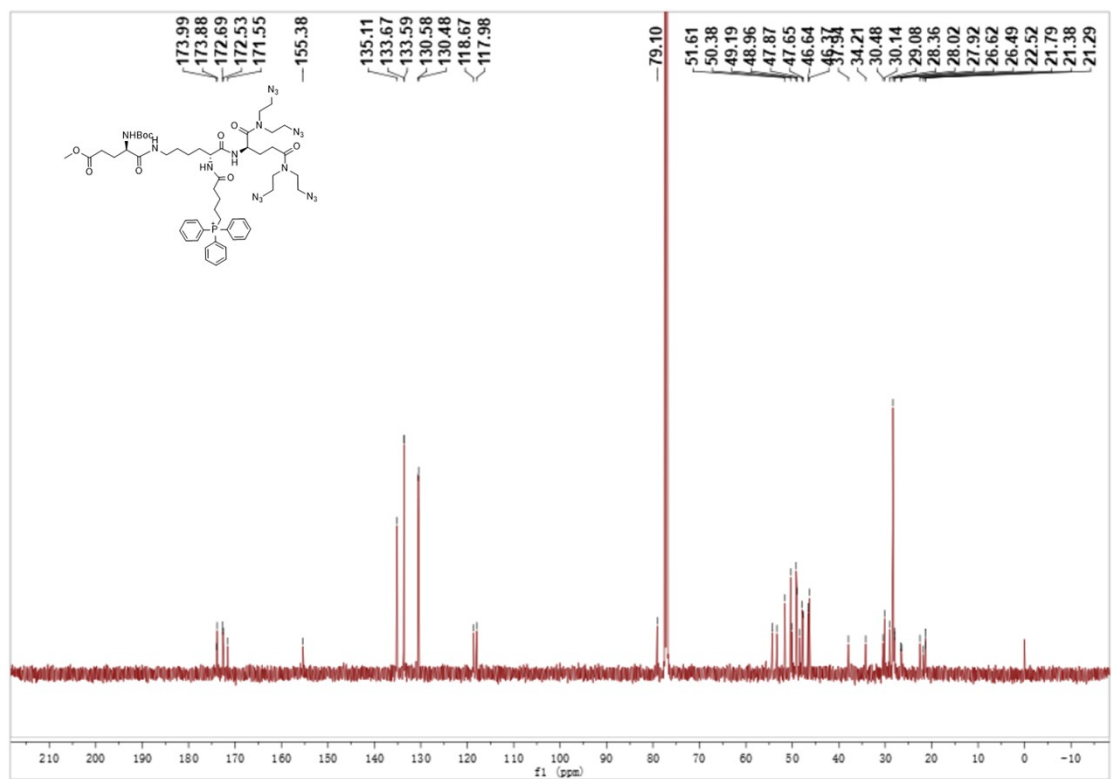


Fig. S18 ^{13}C NMR spectrum of compound 6 (CDCl_3).

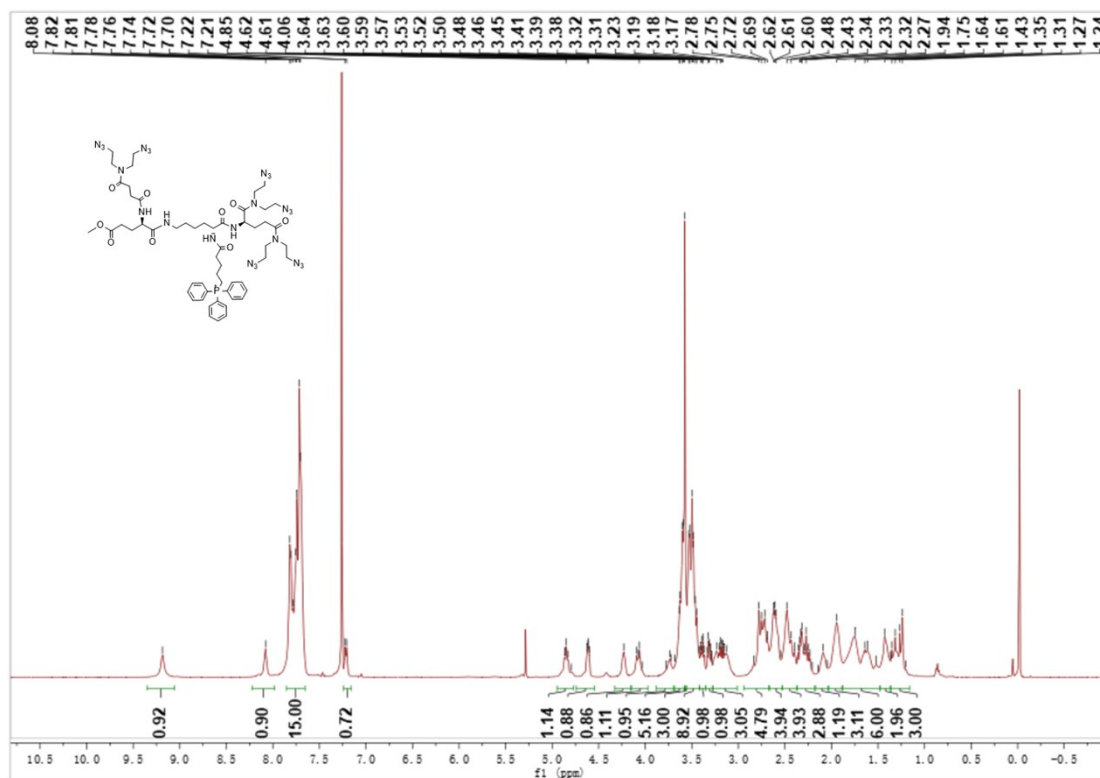


Fig. S19 ^1H NMR spectrum of compound 7 (CDCl_3).

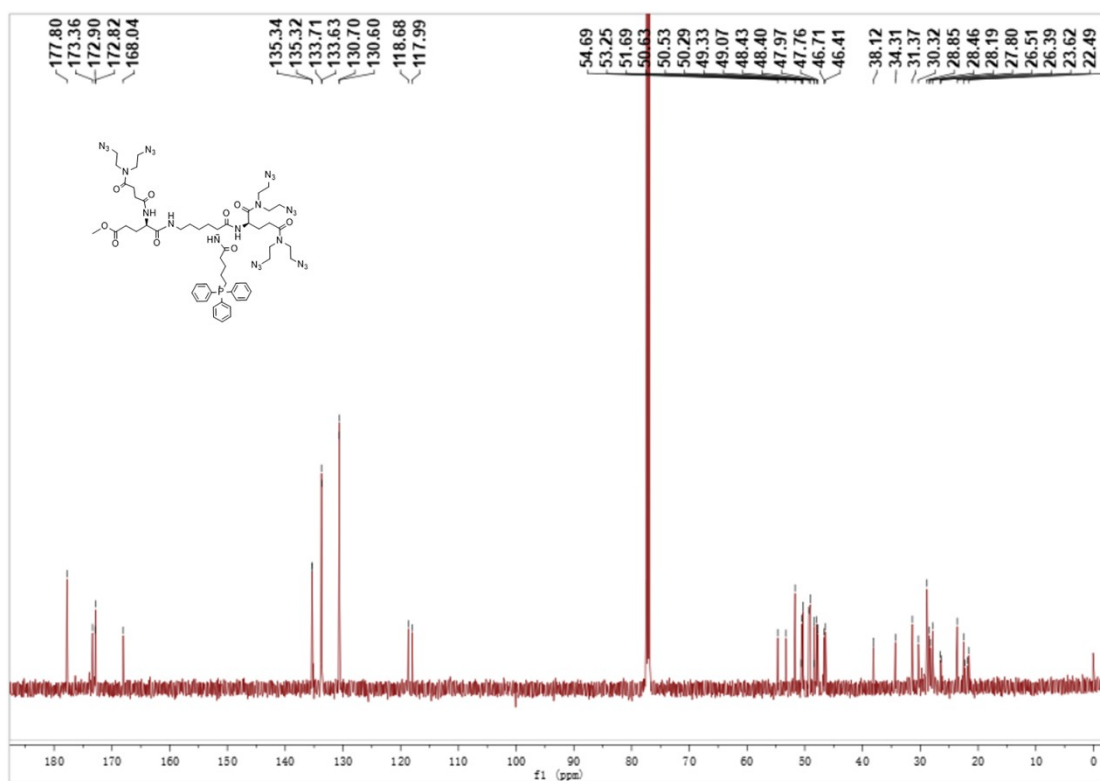


Fig. S20 ^{13}C NMR spectrum of compound 7 (CDCl_3).

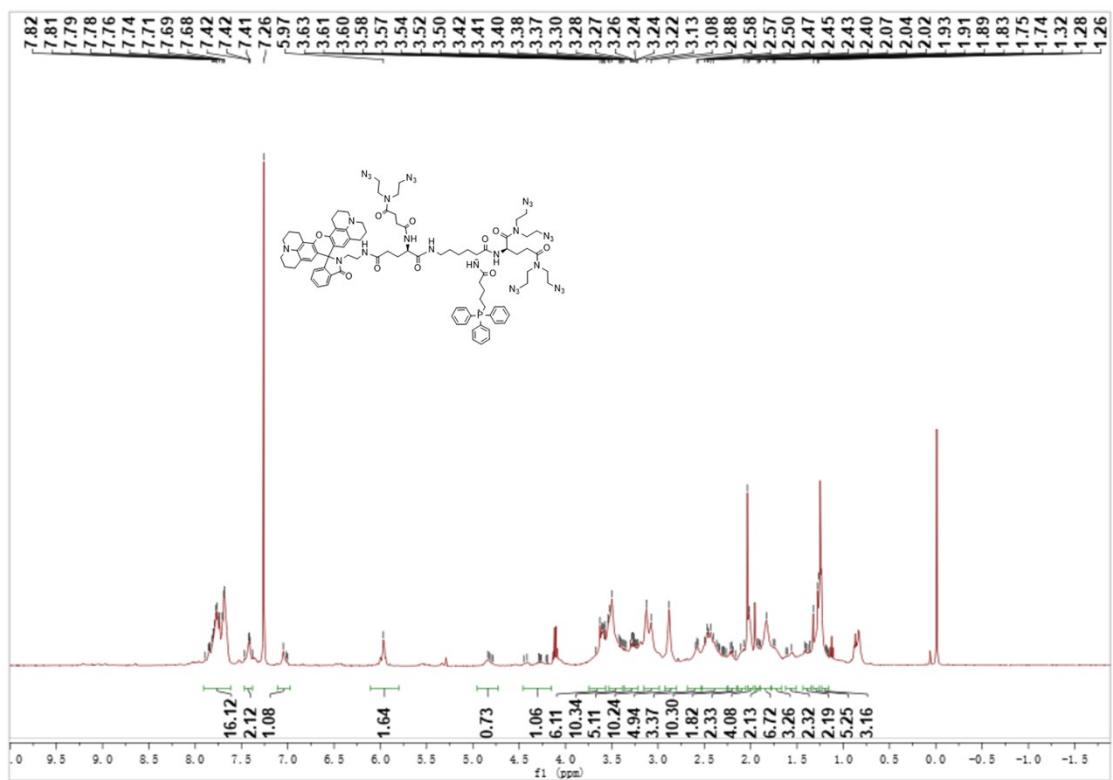


Fig. S21 ^1H NMR spectrum of 6AzProRed-TPP (CDCl_3).

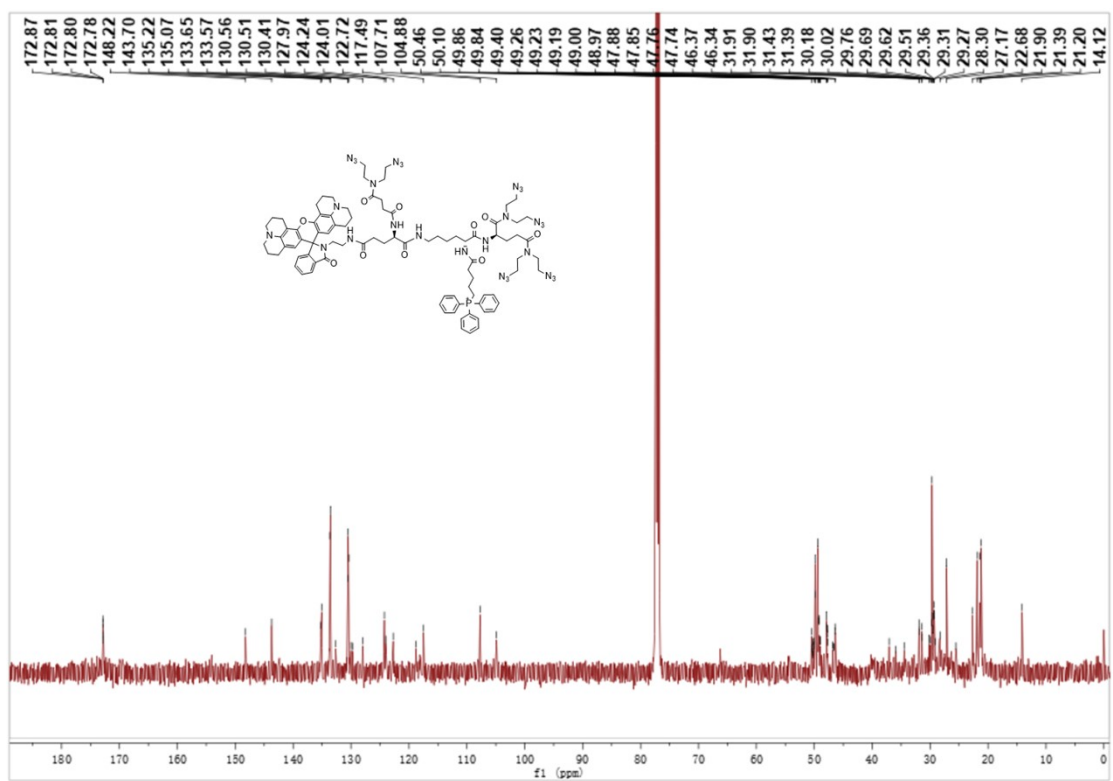


Fig. S22 ^{13}C NMR spectrum of 6AzProRed-TPP (CDCl_3).

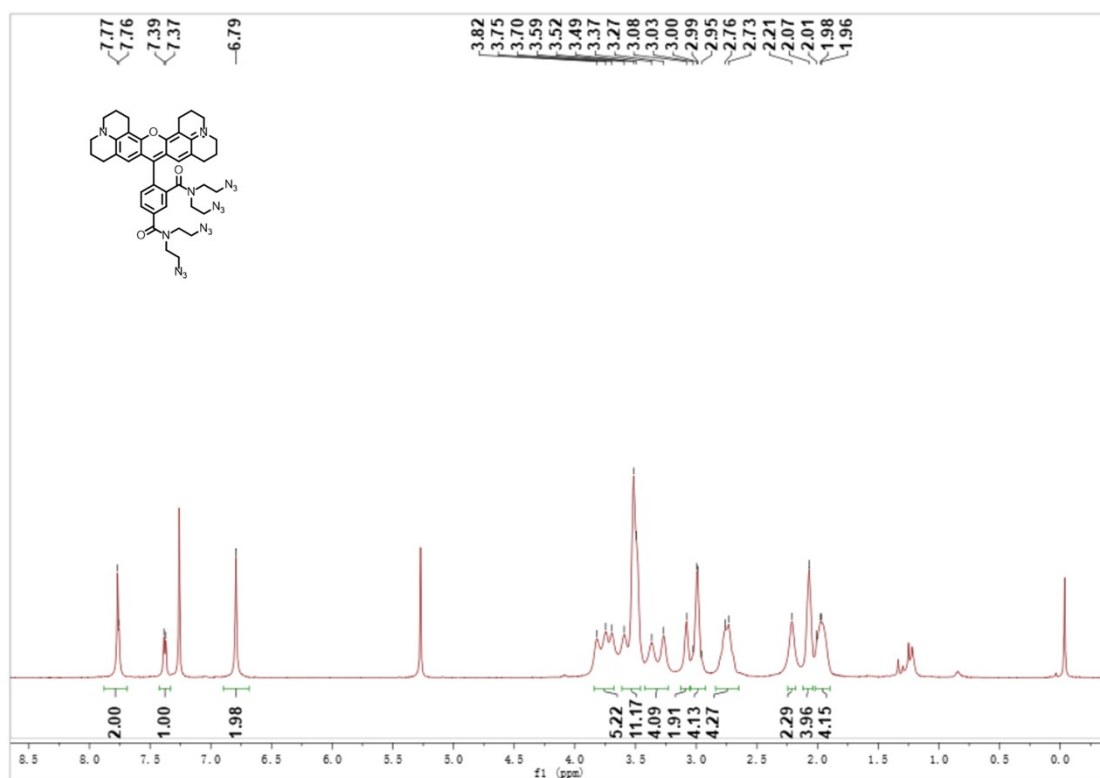


Fig. S23 ¹H NMR spectrum of ⁴AzRed (CDCl₃).

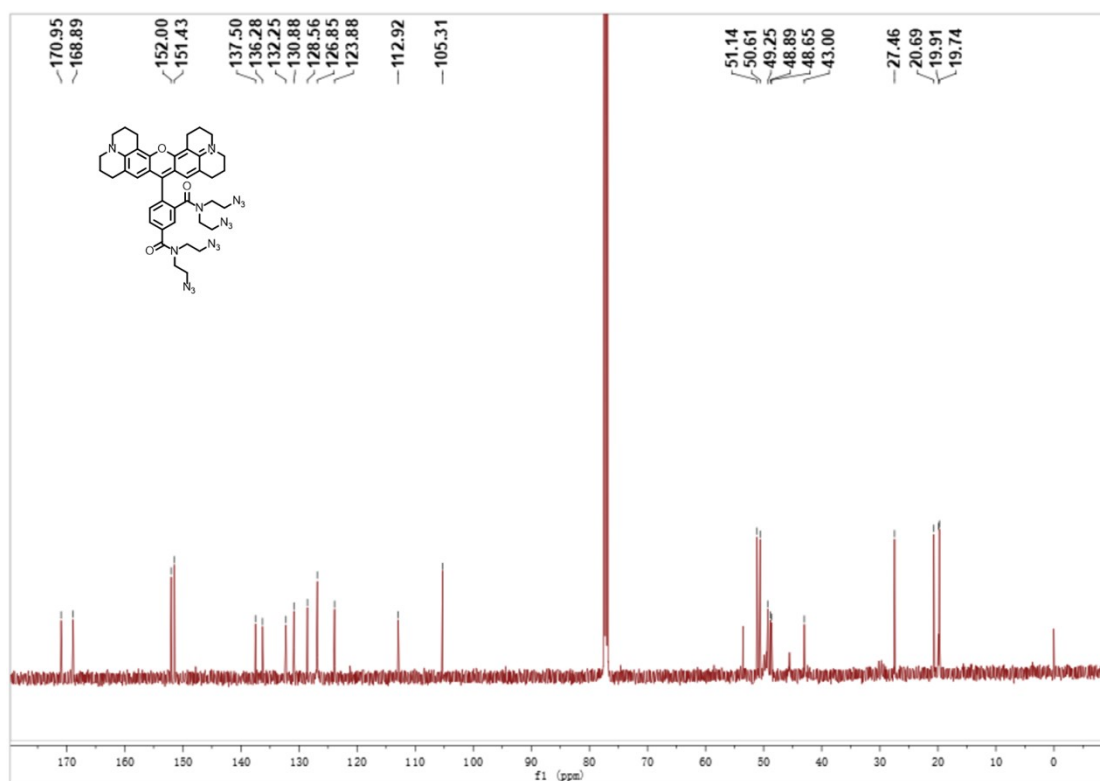


Fig. S24 ¹³C NMR spectrum of ⁴AzRed (CDCl₃).

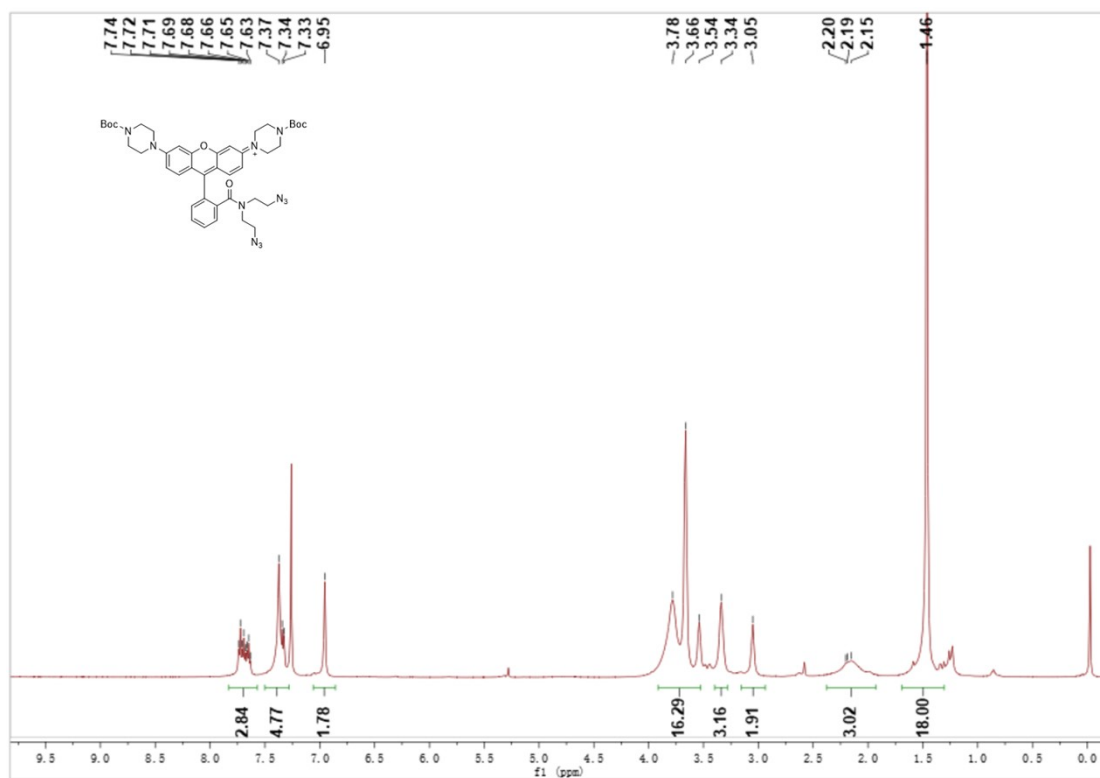


Fig. S25 ^1H NMR spectrum of compound **9** (CDCl_3).

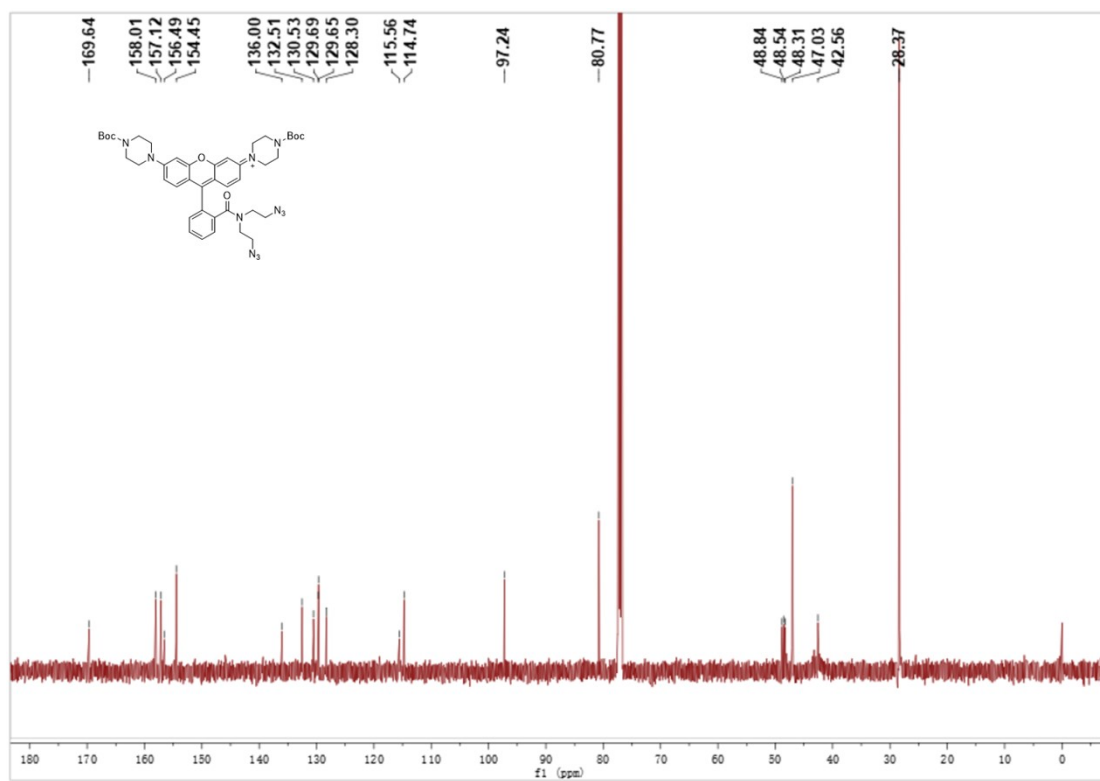
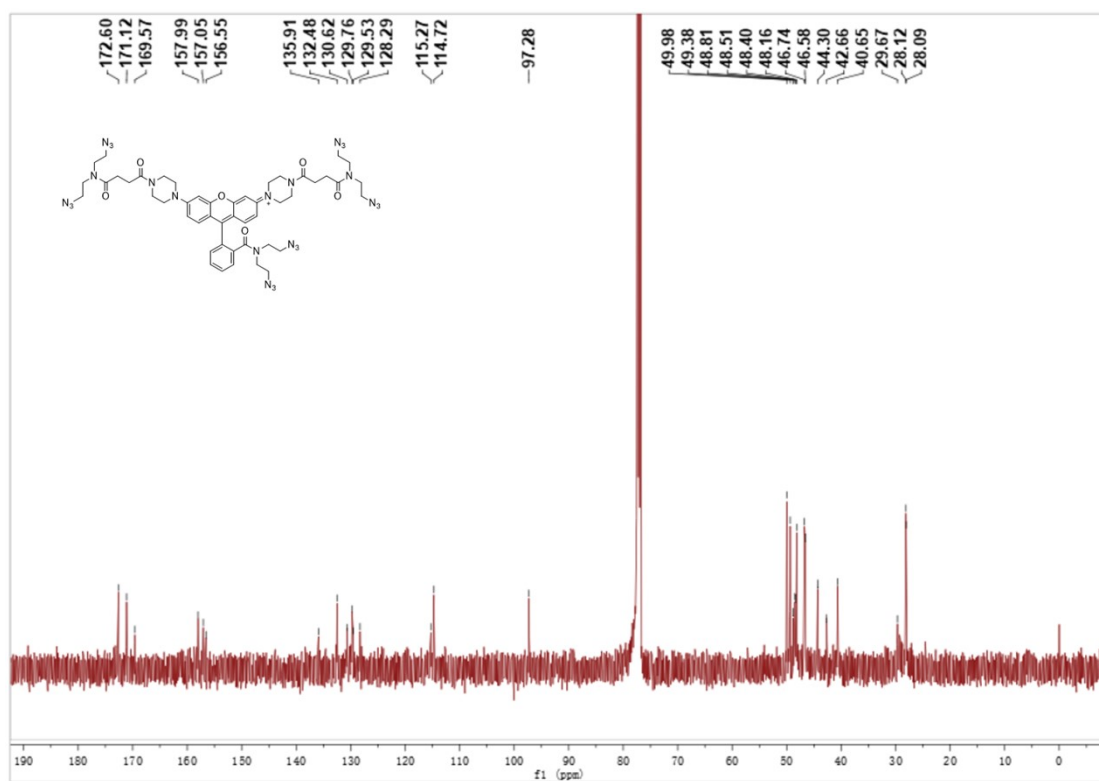
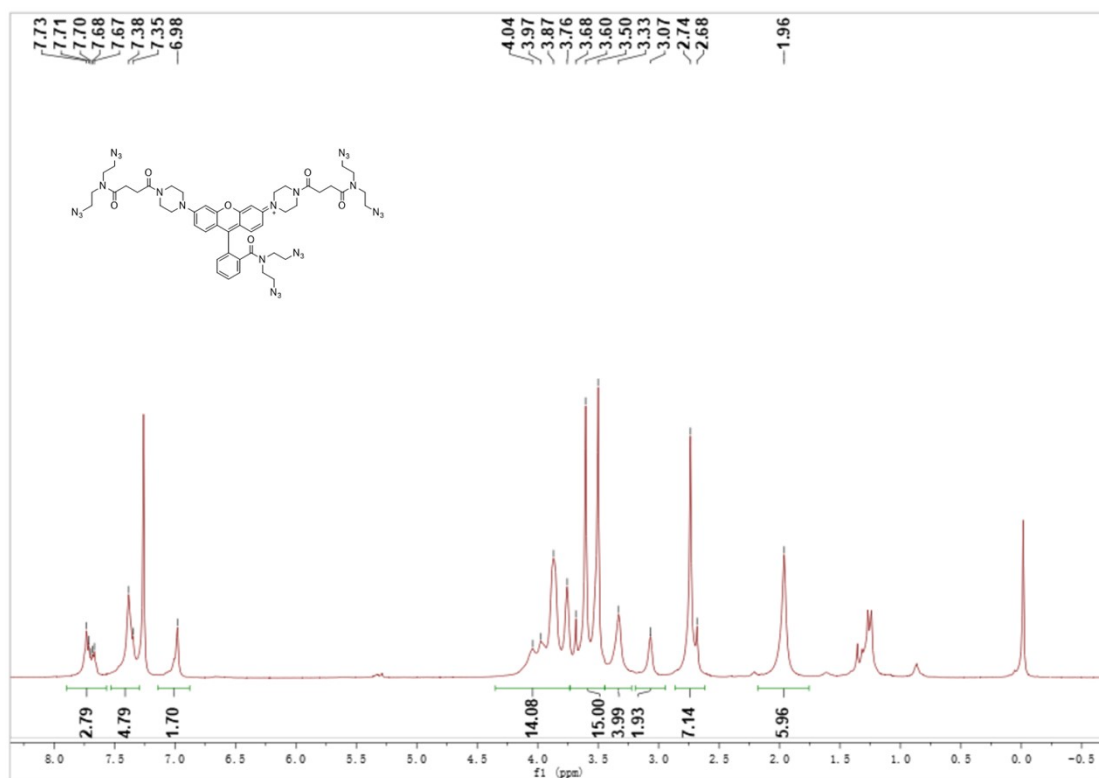


Fig. S26 ^{13}C NMR spectrum of compound **9** (CDCl_3).



Mass spectra

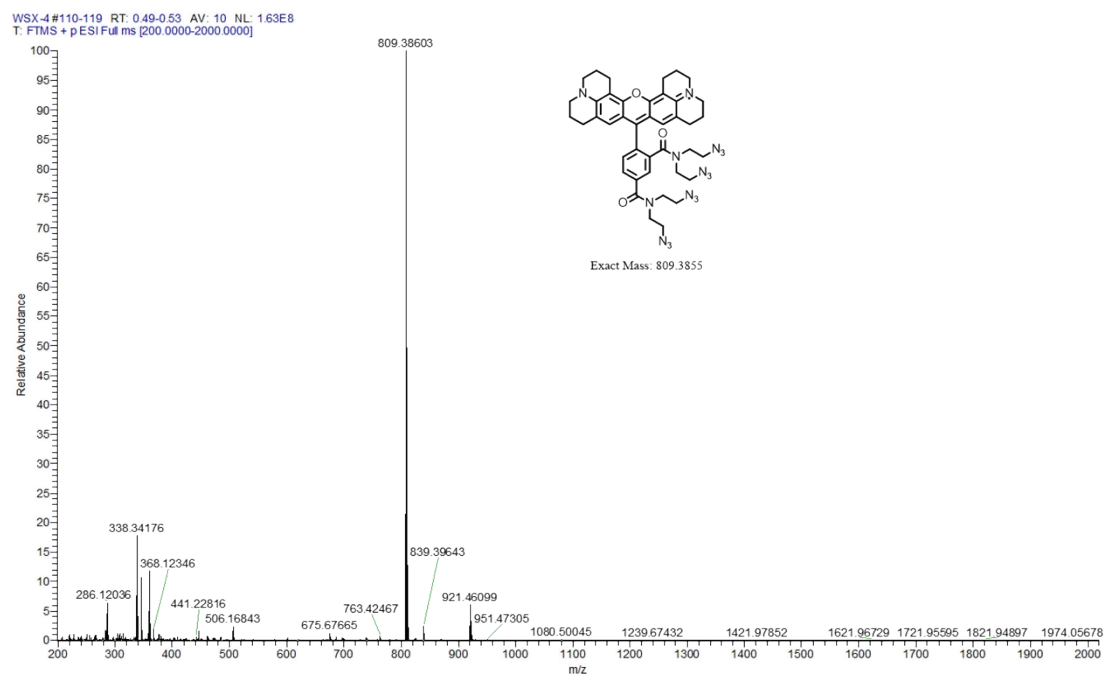


Fig. S29 HRMS of ⁴AzRed.

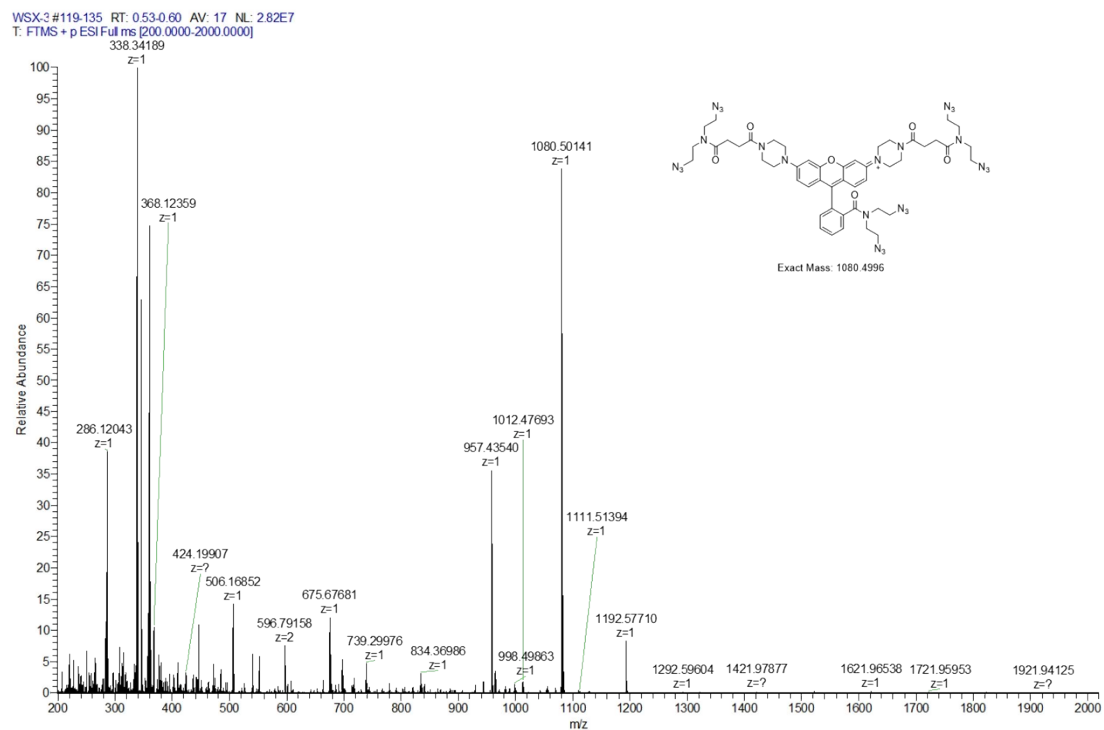


Fig. S30 HRMS of ⁴AzRed.

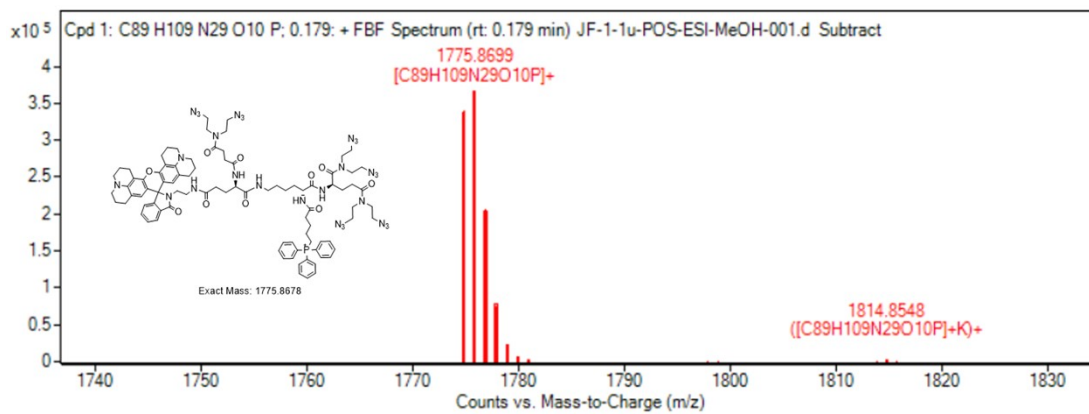


Fig. S31 HRMS of ⁶AzProRed-TPP.